K225: Positron Lifetime in Metals, $\beta^{\pm}$ annihilation

Kanhaiya Gupta and Chelsea Maria John
Rheinische Friedrich-Wilhelms Universität Bonn.
Supervised by Yannick Wunderlich

March 22, 2020

The structure of a solid metal consists of a closely packed metal ions, arranged in a regular way to form a metalic lattce structure. They consists of defects such as vacancies, intersititials mixed dislocations etc. The annihilation radiation from electron-positron pairs has been most successful in monitoring changes in the defects properties as a function of temperature, pressure or anneling treatments. Here, in this experiment we study the defects in Indium metals using positrons annihilation technique from the beta decay of radiocative ^{22}Na.

Keywords: Positron, Annihilation, Lifetime, Defects, Trapping model, Photomultiplier tube

CONTENTS

I. Introduction 1

II. Theory 1
A. Positon annihilation 2
B. Positronium and pickoff decay 2
C. Defects in metals Principles of Positrons Annihilations 2
D. Trapping model and vacancy formation enthalpy 3

III. Experiment 3
A. Experimental setup 3
1. LYSO scintillation crystal 4
2. Photomultiplier 4
3. Single-channel analyzer 5
4. Constant-fraction discriminator 5
5. Fast-slow coincidence circuit 5
B. Measurement process 6
1. Adjustment of the slow circuit 6
2. Adjustment of the fast circuit 6
3. Time calibration measurements 6
4. Measurements of positron lifetime spectra in indium for different temperatures 7

IV. Analysis 7
A. Mean lifetimes at different temperatures 7
B. Enthalpy of the vacancy formation 9

V. Results Conclusions 10

VI. Acknowledgments 10

References 10

I. INTRODUCTION

The use of annihilation radiation from positron-electron pairs to the study the nature of defects in metals has gained significant importance over the past two decades. The most success has been in monitoring changes in the defects properties as a function of temperature, pressure or anneling treatments. In our experiment, defects and the thermal vacancy formation was studied by the positron annhilation technique in Indium at varying temperatures[1].

II. THEORY

Positrons are antiparticles of electrons with same mass, spin but negative charge. There are several possible ways in which positrons can be produced. One of these ways is through the beta β^+-decay of radioactive isotopes. A large majority of investigations on solids by positrons have been done with ^{22}Na, ^{58}Co and ^{86}Sr positron sources, mainly because of their low production costs, simplicity of their manufacture in laboratory and relatively convenient half-life[2].

$$^{22}Na \rightarrow ^{22}Na + e^+ + \nu_e + \gamma \tag{1}$$

In our experiments, the radioactive isotope ^{22}Na is used as a positron source. It has relatively long half-life of 2.61 years and decays in 90.4% of times through eqn(1) emitting a prompt 1.274 MeV -ray simultaneously with the positron birth. The decay scheme of ^{22}Na is shown in Figure 1.

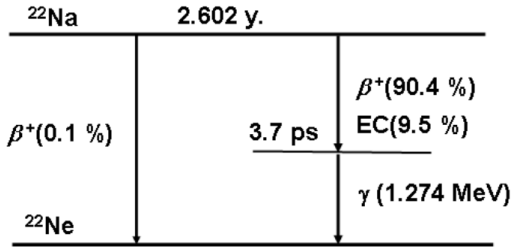

FIG. 1. Decay scheme of the radioactive isotope ^{22}Na. 90.4 % of the isotope decays by emission of a positron and an electron neutrino to the excited state of ^{22}Ne. The ground state is reached after 3.7 ps by emission of a photon of 1.274 MeV. Competitive processes with lower probabilities are electron capture (EC) and direct transition to the Ne ground state.
Source Instruction manual for K225 experiemt[1]

A. Positon annihilation

When a positron and an electron interact through a head-on collision, they annihilate, converting all of their mass into energy (as per Einstein's equation $E = m_o c^2$). The total amount of energy released when a positron and an electron annihilate is 1.022 MeV, corresponding to the combined rest mass energies of the positron and electron. The energy is released in the form of photons. The number of photons depends on exactly how the positron and electron annihilate. Positrons usually have a very short life in a material for the following reasons:

- They can either freely annihilate with electrons directly, like a head-on collision in the medium, resulting in the annihilation process. Two photons are then emitted with an energy of 0.511 MeV as

$$\begin{aligned} e^+ + e^- &\rightarrow 2\gamma \\ E_{e^+} + E_{e^-} &= 2m_o c^2 = E_{2\gamma} \end{aligned} \tag{2}$$

  where E_{e^+}, E_{e^-} and $E_{2\gamma}$ are the energy of the positron, electron and the produced photon pairs and m_o is the rest mass of electron.

- In some materials, they form a stable state with an electron which is similar to the hydrogen atom with a binding energy ∼6.8 eV. This is termed positronium (Ps) which also annihilates.

Ps is generally not found in metals, but is found in molecular materials, metals oxides, molecular liquids and gasses and its annihilation parameters reflects the properties of the containing host medium.

B. Positronium and pickoff decay

When positron is slowed down in a medium to energies < 10 eV, it can form Ps. Ps has two types: p-Ps(antiparallel spin) and o-Ps(parallel spin). The p -Ps state decays through 2γ with a lifetime of about 125 ps in vacuum. While the o-Ps state lives much longer (∼142 ns in vacuum) because its self annihilation (intrinsic annihilation) it is through 3γ-photons by which all have energies less than 0.511 MeV. The ratio probabilities of 3γ and 2γ process for normal positron annihilation are 1/137[3].

The lifetime of the o-Ps state may be substantially reduced if the Ps formed in the vicinity of atoms. This reduction may be due to the so called "pick-off" process in which the positron of the o-Ps annihilates with an electron from the material with opposite spin and then annihilates via 2γ decay, or as a result of a transition from o- to p- Ps, a "quenching process", which then quickly annihilates.

C. Defects in metals Principles of Positrons Annihilations

The structure of a solid metal consists of a closely packed metal ions, arranged in a regular way to form a metalic lattce structure. There are different types of defects in metals. The three main types of defects in metals[5] are:

- point defects- due to vacancies, interstitials, and impurity atoms
- line defects- due to fundamental of edge, screw and mixed dislocations
- planar defects-due to grain boundaries, phase boundaries, twinning and stacking faults

When energetic positrons are injected into a solid from an isotope such as ^{22}Na, they rapidly lose almost all their energy by a succession of ionizing collision with electrons and ions of the medium as shown in Fig(2), they are slowed down to thermal energies (∼ 0.27 eV). During this energy loss process, the positron travels a distance into the solid which is larger, the higher its initial energy. Because of multiple scattering events the positron paths are quite tortuous and the ultimate point of thermalization may locate between the surface and a depth defined by the maximum range.

The positron may annhilate promptly with the free electron giving two γ-ray each of energies of 511 keV in opposite direction or it may be trapped in the defects such as vacancies, vacancy agglomerates and dislocations due to formation of attractive potential at the sites. The lifetime of trappled positron increases from that of a delocalized positron due to reduced electron density. The lifetime is best explained by the trapping model.

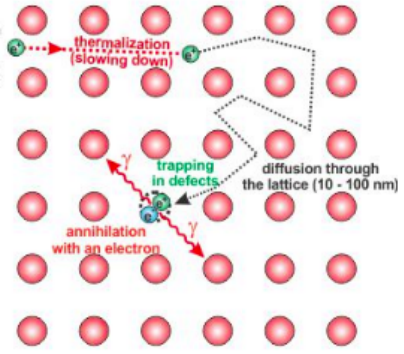

FIG. 2. Schematic diagram shows a single positron penetrating through matter undergo various processes influencing the state from which the positron annihilates with an environmental[6] electron.
Source: https://www.hzdr.de/db/Cms

D. Trapping model and vacancy formation enthalpy

The trapping model[7] describes positron annihilation inside metal as a simple two-state system. Free positrons either annihilate with a rate λ_f or get trapped with rate κ, while trapped positrons annihilate with rate $_t$ The transition rate from the free to a trapped state is thought to be proportional to the defect concentration. The process is described by two coupled differential equation:

$$\begin{aligned} \frac{dn_f}{dt} &= -\lambda_0 n_f - \kappa n_f \\ \frac{dn_t}{dt} &= -\lambda_t n_t + \kappa n_f \end{aligned} \tag{3}$$

where n_f and n_t represent the probabilites that positron is found in the free or the trapped states. Experimentally we don't distinguish between these two types of annihilation and the observable is the sum $W(t) = -dn/dt = -dn_f/dt - dn_t/dt$. Thus the equations are solved by

$$W(t) = \frac{I_0}{\tau_0} e^{\frac{t}{\tau_0}} + \frac{I_t}{\tau_t} e^{\frac{-t}{\tau_t}} \tag{4}$$

where $I_t = \frac{\kappa}{\lambda_f + \kappa - \lambda_t}$, $I_0 = 1 - I_t$, $\tau_t = \frac{1}{\lambda_t}$ and $\frac{1}{\tau_0} = \lambda + \kappa$. Taking into consideration, the finite time resolution of experimental equipment, the measured life time spectrum will be the convolution of the time resolution function.

$$P(t) = \frac{1}{\sqrt{2\pi}\sigma} e^{-\frac{1}{2}\left(\frac{(t-t_0)}{\sigma}\right)^2} \tag{5}$$

and $W(t)$:

$$\begin{aligned} M(t) &= \int_0^t W(p)P(p-t)dp \\ &= \frac{I_0}{2\tau_0} d^{\frac{\sigma^2 - 2\tau_0(t-t_0)}{2\tau_0^2}} \{\, erf(a_0) + erf(b_0)\} \\ &+ \frac{I_t}{2\tau_t} d^{\frac{\sigma^2 - 2\tau_0(t-t_0)}{2\tau_0^2}} \{\, erf(a_t) + erf(b_t)\} \end{aligned} \tag{6}$$

where

$$\begin{aligned} a_0 &= \frac{\sigma^2 + \tau_0 t_0}{\sqrt{2}\sigma\tau_0}, b_0 = \frac{\tau_0(t-t_0) - \sigma^2}{\sqrt{2}\sigma\tau_0} \\ a_t &= \frac{\sigma^2 + \tau_t t_0}{\sqrt{2}\sigma\tau_t}, b_t = \frac{\tau_t(t-t_0) - \sigma^2}{\sqrt{2}\sigma\tau_t} \end{aligned} \tag{7}$$

In actual experiment the data are not normalized and have background noises, therefore we will use the fitting functions:

$$\begin{aligned} N(t) &= \frac{A_0}{2\tau_0} d^{\frac{\sigma^2 - 2\tau_0(t-t_0)}{2\tau_0^2}} \{\, erf(a_0) + erf(b_0)\} \\ &+ \frac{A_t}{2\tau_t} d^{\frac{\sigma^2 - 2\tau_0(t-t_0)}{2\tau_0^2}} \{\, erf(a_t) + erf(b_t)\} + BG \end{aligned} \tag{8}$$

The intensity of trapped positrons is dependent on the density of vaccancies inside the metal, which is a temperature dependent quantity. Positron lifetime analysis can be used to determine the vacancy formation enthalpy H_t. For this purpose we first define the mean life time as

$$\bar{\tau} = I_0\tau_0 + I_t\tau_t = \tau_t \frac{1 + \mu c_t \tau_t}{1 + \mu c_t \tau_t} \tag{9}$$

where $\mu c_t = \kappa$ and c_t is the concentration of vacancies which depends on temperature as

$$c_t = e^{(S_t T - H_t)/kT} \tag{10}$$

Therefore

$$\bar{\tau} = I_0\tau_0 + I_t\tau_t = \tau_f \frac{1 + \mu e^{\frac{S_t}{k}} e^{-\frac{H_t}{kT}} \tau_t}{1 + \mu e^{\frac{S_t}{k}} e^{-\frac{H_t}{kT}} \tau_f} \tag{11}$$

With the known value $\mu e^{\frac{S_t}{k}} = 10^8 ns^{-1}$, it is possibe to determine τ_f by fitting equation 11 to the calculated mean lifetime at different temperatures. Once τ_f is obtained, it is easy to determine H_t by linear fitting after taking the logarithm

$$\mu c_t = \frac{\bar{\tau} - \tau_f}{\tau_f(\tau_t - \bar{\tau})} \tag{12}$$

III. EXPERIMENT

A. Experimental setup

To measure the positon lifetime the fast-slow coincidence circuit joined with the multichannel

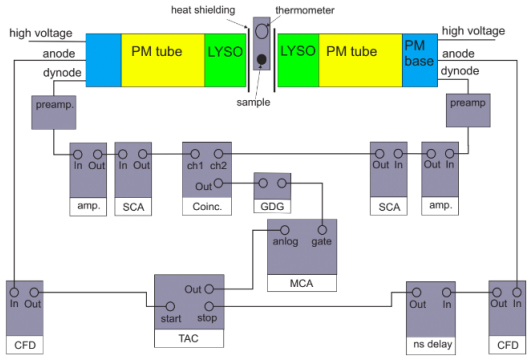

FIG. 3. Fast-slow coincidence circuit used in the experiment. Slow circuit consists of CGF and nonoseconds delay (ns for one of the branches) Slow circuit is connected to the MCA through coincidence module and gate fast circuit through time to amplitude converter (TAD).
Source: Instructions for K225 experiment

analyzer(MCA) was used which is shown Figure 3.

To determine the γ-rays from ^{22}Na decay and from the positron annihilation in indium metal, scintillation detector with LYSO crystal, shown in Figure 4 was used.

1. *LYSO scintillation crystal*

Lutetium-yttrium-oxyorthosilicate ($Lu_{1.8}Y_{.2} - SiO_5 : Ce$) is a Lutetium based Cerium doped semiconuctor used as scintillation material. It has a number of advantages such as high density, short decay time, non-hygroscopicity. It has improved light output and better energy resolution.

As mentioned before, LYSO is a Lutetium based scintillator, it contains radioactive isotopes ^{176}Lu which undergoes a β^+ decay into ^{176}Hf. It decay scheme is shown is Figure 5.

The principle of operation of scintillators is based on the electronic band structure of semiconductors. When a photon emitted by a source falls on a scintillator, it excites one of th electrons in the valence band so that this electron can cross the gap and enter the condictivity band. In the conductivity band the excited electron can either emit a single photon and return back to the valence level, or first collide with neighbouring electrons therefore forcing them to emit several photons and then fall into the valence band. In this way one or several photons get emitted -a scintillation occurs.

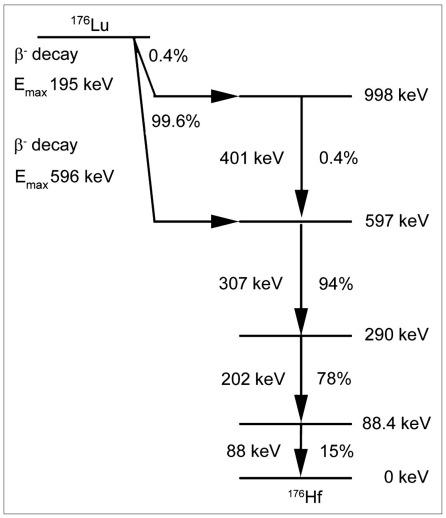

FIG. 4. Decay scheme of ^{176}Lu showing β^- emission followed by cascade of prompt $\gamma - ray$ emissions. All intensities are relative to number of decays of ^{176}Lu.[8]

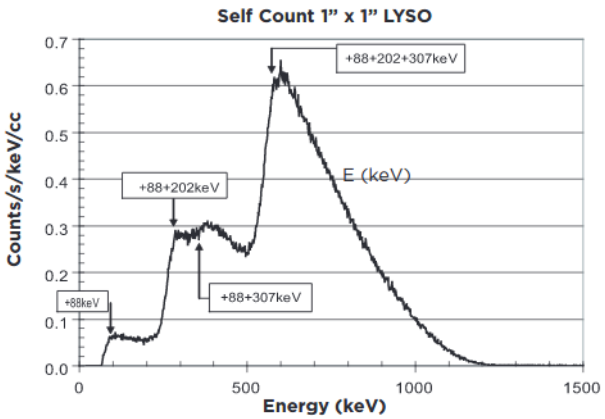

FIG. 5. LYSO is a Lutetium-based scintillator which contains a naturally occurring radioactive isotope ^{176}Lu, a beta emitter. The decay results in a 3 gamma ray cascade of 307, 202 and 88 keV, where self-absorption of these photons results in the above spectra in a 1" × 1" cube. Total rate for this activity is 39 cps/g [8]
Source: https://www.crystals.saint-gobain.com/products/

2. *Photomultiplier*

A photon emitted by a scintillation material reaches the photomultiplier tube (PMT), as shown in Figure 7. When the photon strikes the photocathode, a photoelectron is emitted. This electron is focused onto the electron-multiplier section which consists of several dynodes. A dynode is an electrode which , when stoke by a single electron, emits several electrons. Each of the dynodes is held at a more positive potential than the previous one, so that the emitted electrons are accelerated to strile the next dynode and emit more electrons. When the avalanche of electrons

reaches the anode, a sharp pulse is produced. This signal can be easily detected and used for further analysis. In our experiment however, because of large amplification in the PMT, input of a slow branch of the fast-slow circuit is connected not to the anode, but to the last dynode of PMT so that height of the signal can be analysed. The input of the fast branch is conneted to the anode.

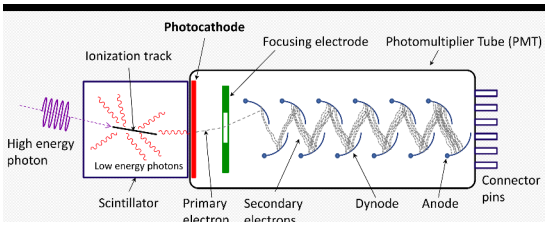

FIG. 6. Schematic of a photomultiplier tube coupled to a scintillator. This arrangement is for detection of $\gamma - rays$.[9]
Source: https://en.wikipedia.org/wiki/Photomultiplier

3. *Single-channel analyzer*

Single-channel analyzer (SAC) is used to analyze the signal's amplitude. It has two adjustable parameters - lower bound E and window δE. When the peak of the incoming signal falls inside the window, a output pulse is produced. In this way SCA transforms the incoming analog signal, whose height falls between E and δE, into digital logic signal.

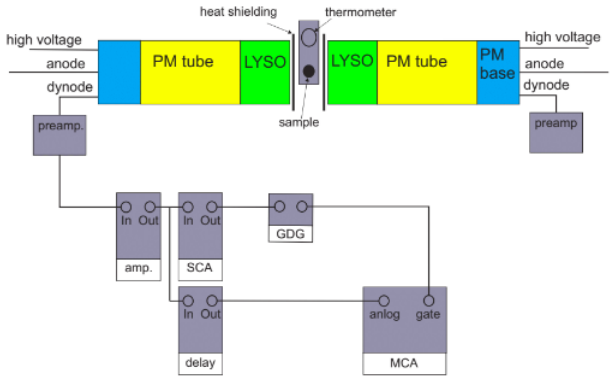

FIG. 7. Adjustment of the SCA windows. Here just one side is shown. The adjustments have to be done for each side separately
Source: Instructions for K225 experiment

4. *Constant-fraction discriminator*

Constant-fraction discriminator (CDF) generates an output signal at a constant fraction of the incoming signal, so that the response time of CFD doesnot depend on the incoming signal's height and allows to produce a walk-free timing signal. Walk is an effect caused by the variation in the amplitudes of incoming signals. If we consider two coincident signals of the same shape and same rising time and trigger them to some particular height, we will notice the outgoing signal to "walk" in time, because the height, necessary to produce the outgoing signal, will be reached first by the signal with the bigger amplitude and the one by the smaller one. This is undesirable effect if we want to have good timing resolution. CFD opperates by first splitting the incoming signal into two. Then one of them is delayed by the time that it takes the signal to rise from the constant fraction κ. Finally, the two parts are summed, producing a bipolar signal. The point at which the resulting signal crosses zero (signals cancel each other) is at the constant fraction κ of the initial signal. Even though this technique allows to produce the logical signal not dependent on the height of the incoming signal, there is still walk caused by the time jitter -noise and statistical fluctuations in the detector signal.

5. *Fast-slow coincidence circuit*

To provide a good timing and pulse-height resolution ,a fast-slow circuit wired as shownn in Figure 8 is used. The fast-slow circuit, as indicated in its name, consists of a slow and fast branch that are connected to MCA.

The slow circuit analyzes the height of the signal coming from dynode. It consists of a preamplifier, an amplifier and SCA. Two slow circuits are then connected through a coincidence module and gates to the MCA. MCA counts the number of pulses with different heights and stores this number in the multichannel memory.

One of the fast brances - the one that analyzes the signal from the 1274 keV photon emitted during ^{22}Na decay - consists of a CFD. The other fast branch analyzes the signal from the 511 keV photon emitted in the annihilation process of positron and electron in indium. This branch are joined in the time-to-amplitude converter (TAC) that converts the time between the two logic pulses into an output signal, whose amplitude depends on the time. The signal from TAC goes to the MCA.

B. Measurement process

1. *Adjustment of the slow circuit*

At first the gain of the main amplifiers has to be adjusted. Therefore each detector is set up separately as shown in Figure 7. The output of the SCA is used as a gate for the MCA. Therefore the signals have to be checked for simultaneousness, so that the analog signal peak is located inside of the gate signal. After these adjustments an intrinsic LYSO energy spectrum and the spectrum of a ^{22}Na source is acquired.

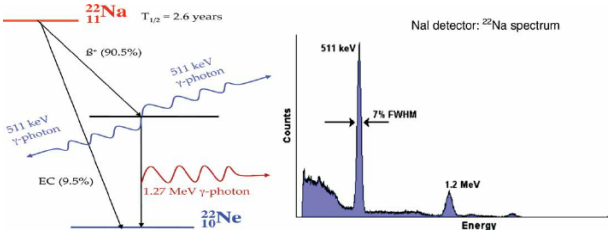

FIG. 8. ^{22}Na spectrum: the first peak is 511keV corresponds to the annihilation of a positron, emitted during beta-decay of natrium, with electron, the second peak correspons to the emission of 1274 keV photon by an atom of ^{22}Na when it transmits from the excited state to the ground state[10].

The structures visible in the decay scheme are identified and the gain of the main amplifier is adjusted in order to cover the 1275 keV line. Remark: Whenever the gain is changed from now on, the SCA windows need to be adjusted accordingly. In order to be able to determine the lifetime one needs to calibrate the time scale. To prepare the time calibration measurement the setup has to be adjusted to detect the rays of a simultaneous event. For this both SCA windows have to be set around the 511 keV lines in order to define the annihilation of an electron positron pair. After setting up the first detector, the procedure was repeated with the other side too.

2. *Adjustment of the fast circuit*

As a next step, the thresholds of the CF discriminators need to be adjusted. The aim is to set the threshold as low as possible in order to have a good acceptance but at the same time cut away noise which would pollute the spectrum. There are different options to optimise thresholds. We were suggested to look at the signals of one of the slow branch and CFD on the oscilloscope. After the CFD thresholds of both detectors have been adjusted, the time delay between the start and stop signal has to be set. Therefore connect the CFD outputs with the oscilloscope and use the ns delay to adjust the time delay to ca. 20 ns. Now connect the start and stop signals to the TAC, and set the time range of the TAC to 50 ns. Use the same cables to connect to the TAC as used on the osciloscope. If the TAC provides an output signal, the fast circuit is prepared.

3. *Time calibration measurements*

On adjusting both the slow and fast circuits and setting the SCA's window to cover the 511 keV regions, the output signals are connected to the coincident module and checked for coincidence. The output from TAC and coincidence module is also checked for simultaneousness. Then the outputs are connected to MCA.

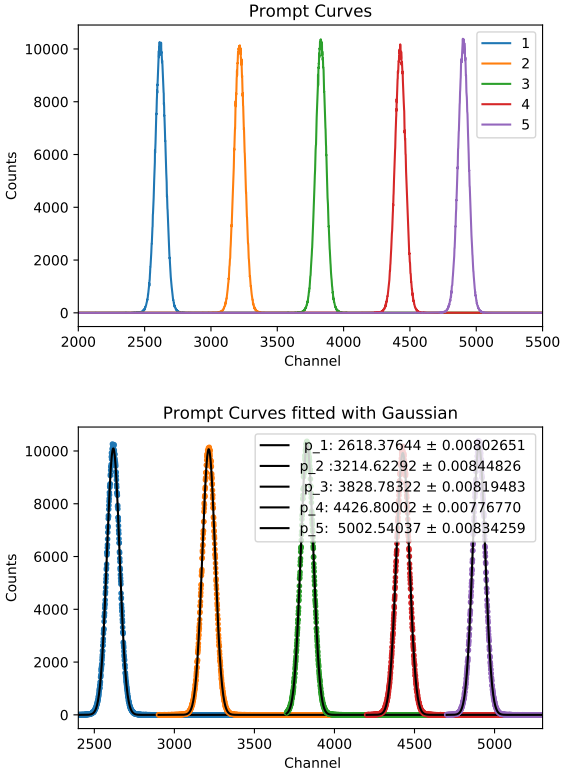

FIG. 9. Prompt curves and the gaussian fitted prompt curves for the time calibration measurements

In order to do time calibration, five spectra are measured with counts up to 10,000 with a time delay of 4ns between them. The counts are taken up to 10,000 so that the statistical uncertainty is less than 1% Each of these five spectrums is fitted with Gaussian curves and the mean channel value is found out.

Using the above Table I , a linear plot was made to determine the number of channels for a time period of 1ns and it was found to be

$$n = \Delta channel = 149.56 \pm 0.92 ns^{-1}$$

Mean Channel (x_0)	Time delays(ns)
2618.3764 ±0.0080	4
3214.6229 ±0.0084	8
3828.7832 ±0.0082	12
4426.8000 ±0.0078	16
5002.5404 ±0.0083	20

TABLE I. Fitted prompt peak mean values vs the corresponding time delay

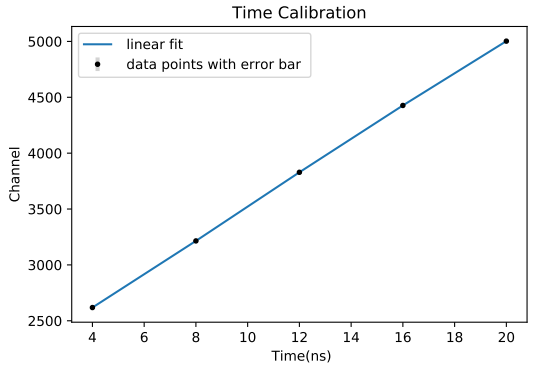

FIG. 10. Linear fit of the time calibration of MCA-channels

The error bars are too small to be visible in the plot and it comes from the uncertainties in the peak value and that of the slope in the linear fit.
The time resolution from the time calibration is found to be:

$$\sigma = (0.3845 \pm 0.0004)ns$$

So now we know that the lifetimes will be of the order of the time resolution.

4. *Measurements of positron lifetime spectra in indium for different temperatures*

To get the spectra of positron at different temperatures in Indium the window of the SCA connected to the detector with no delay in the fast circuit has to be adjusted to cover the 1.274MeV region. Now the two branches of the fast-slow coincidence circuit measures the starting signal (1.274MeV) and the other two measures the stop signal of 0.511MeV from the annihilation of electron and positron. The temperature of the Indium sample is adjusted using a potentiometer and the value is read off from a digital thermometer. In order to find the time taken to stabilize within 1K temperature, the heat constant of the heating system was found. It was done by changing the temperature and recording it every 30 sec until it stabilized within 1K. On plotting the heat curve we found that it takes 21 min for the temperature to stabilize. This long time duration maybe because the systematic error from the thermometer and the heating system.

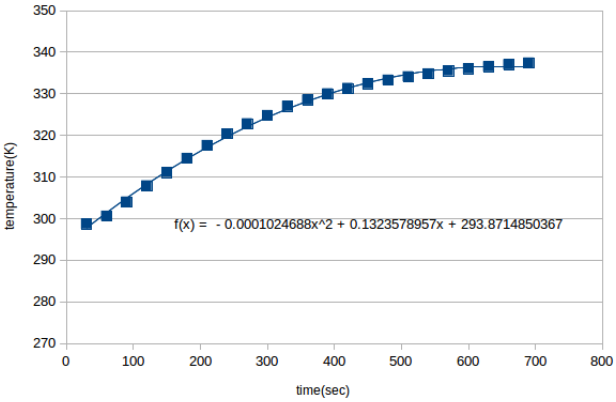

FIG. 11. Heating curve for the heating system used in the experiment

We took readings starting from close to room temperature and measured the spectra for the following 7 temperatures – 298.75K, 340.25K, 350.65K, 365.25K, 378.25K, 392.25K and 400.85K. The spectrum was recorded for time duration of 30 minutes.

IV. ANALYSIS

In this section, we analyse the data acquired at seven different temperatures and extract the information regarding the temperature dependency of vacancy formation.

A. Mean lifetimes at different temperatures

Each of the seven spectrums is fitted with equation (8) using lmfit in python and the parameters τ_0, τ_t, A_0 and A_t are determined from the fit. The plot of the spectrum with their fitting are shown in Figure 12. The number of counts is measured against the MCA channel, but it is further calibrated into time and plotted.

From A_0 and A_t further I_0 and I_t are also calculated. The mean life time is then calculated using the equation(9). The following Table 2 contains the values for the lifetimes and the intensities.

The errors of the parameters were given by the fitting program while the error for relative intensities and mean lifetime were calculated separately using equation (14) 15 respectively. The temperature dependence of lifetime τ_0 ,τ_t and relative intensities I_0 and I_t can be seen below.

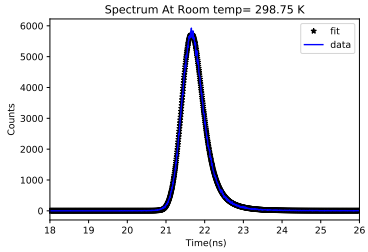

Spectra at T = 298.75K

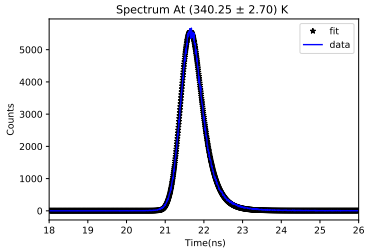

Spectra at T = 340.25K

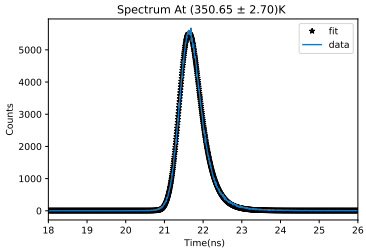

Spectra at T= 350.65

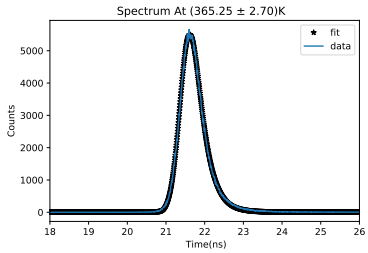

Spectra at T = 365.25K

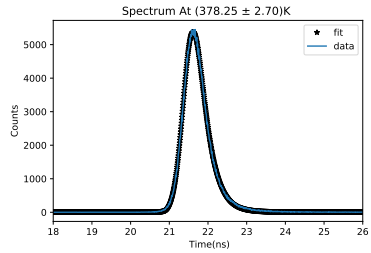

Spectra at T = 378.25K

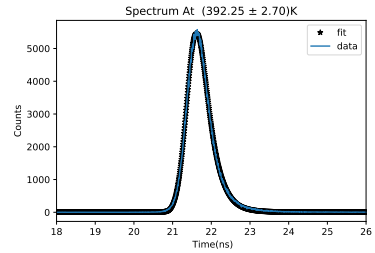

Spectra at T = 392.25K

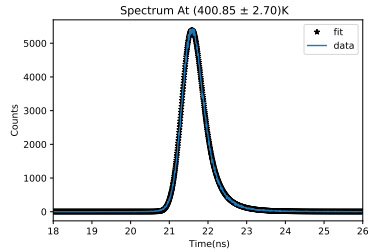

Spectra at T = 400.85K

FIG. 12. Lifetime spectra of positron in Indium, measured for seven different temperatures starting from the room temperature. Number of counts were initially measured against channel of MCA, but were then calibrated into time.TThe blue line on the graph represents the fitted curve given by equation (8).

T(K)	$\Delta T(K)$	$\tau_0(ns)$	$\Delta\tau_0(ns)$	$\tau_t(ns)$	$\Delta\tau_t(ns)$	$I_0\%$	ΔI_0	$I_t\%$	ΔI_t	$\bar{\tau}(ns)$	$\Delta\bar{\tau}(ns)$
298.75	2.7	0.2842	0.0012	0.382	0.0013	87.3040	0.1838	12.6990	0.1838	0.3530	0.0906
340.25	2.7	0.2717	0.0014	0.372	0.0013	86.2565	0.1807	13.7434	0.1807	0.3542	0.0869
350.65	2.7	0.2614	0.0014	0.374	0.0014	85.9649	0.1899	14.0350	0.1899	0.3568	0.0906
365.25	2.7	0.2587	0.0014	0.378	0.0014	83.9886	0.1742	16.0114	0.1742	0.3612	0.0845
378.25	2.7	0.2422	0.0015	0.3714	0.0012	83.8978	0.1732	16.1022	0.1732	0.3645	0.0817
392.25	2.7	0.2342	0.0014	0.3837	0.0013	83.2073	0.1684	16.7927	0.1684	0.3689	0.0808
400.85	2.7	0.2281	0.0015	0.3844	0.0014	82.7810	0.16685	17.2190	0.1669	0.3731	0.0799

TABLE II. Lifetimes and relative intensities obtained from the fit to the lifetime spectra at different temperatures.

Spectrum at Temp	Reduced χ^2
T = 298.75K	0.93
T = 340.25K	0.94
T = 350.65K	0.93
T = 365.25K	1.04
T = 378.25K	0.94
T = 392.25K	0.91
T = 400.85K	0.95

TABLE III. Reduced χ_2 values of the fitted spectrum

$$\Delta I = \Delta_0 = \Delta_t = \frac{\sqrt{(A_1\Delta A_0) + (A_0\Delta_t)}}{(A_0 - A_t)^2} \quad (13)$$

$$\Delta\bar{\tau} = \sqrt{(\tau_0^2 + \tau_t^2)\Delta I^2 + (I_0\Delta\tau_0)^2 + (I_t\Delta\tau_t)^2} \quad (14)$$

The lifetime of free positron is lower than lifetime of trapped positron which is as expected, since on being trapped the interaction probability with surrounding electrons is far reduced than that of free positron. Further from Figure 12, it can be seen that τ_t is fairly constant with the temperature

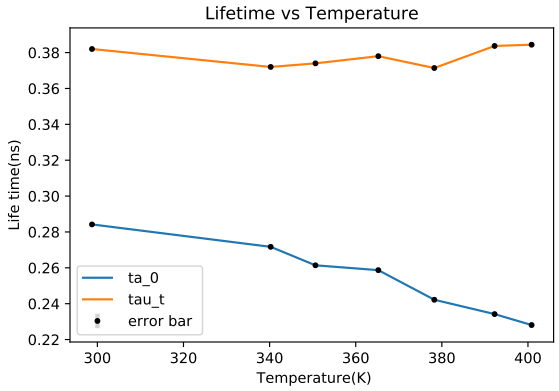

FIG. 13. Lifetimes τ_0, related to the lifetime of free positron, and τ_f- lifetime of a positron trapped in a defect

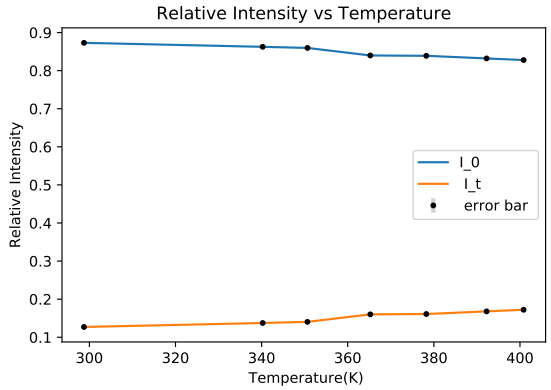

FIG. 14. Intensities I_0 and I_t. that specify the probabilities of detection of free and trapped positrons respectively, are used to calculate $\bar{\tau}$

region in this experiment, which supports our assumptions of the two-state trapping model that τ_t is independent of temperature. τ_0 decreases with temperature which can be explained as the temperature increases there is an increased rate of collisions between positron and electron and hence lesser lifetimes.

From the Figure 13, it can be seen that the relative intensity I_0 decreases slightly as the temperature increases where as I_t increases with temperature. It can be also seen that I_0 is larger than I_t . This means than the probability of a positron getting trapped is lesser than being free and it increases with temperature. It can be related to the number of defects in Indium at temperatures below melting point being lesser and hence the probability of being trapped is less.

The mean life time depends on temperature as a sigmoidal(S-curve) curve as seen from equation (9). On fitting the calculated mean life time with the S-curve the following graph shown in Figure 14, is obtained: In this fitting $\mu exp(S_t/K)$ is taken

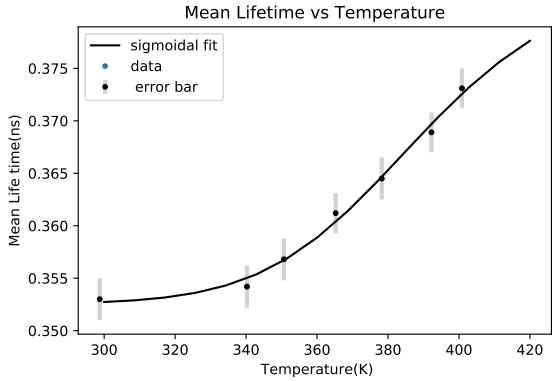

FIG. 15. Sigmoidal fit to the positron mean lifetime done for determination of the free and trapped positron lifetime τ_f and τ_t

as $10^8 ns^{-1}$ from the literature[11] and the free parameters are τ_f,τ_0 and H_t. The fitting gives the following values:

$$\tau_f = (0.35260.0013)ns$$
$$\tau_t = (0.38460.024)ns$$
$$\frac{H_t}{k_B} = (6762 \pm 178)K$$
$$H_t = (0.58260.0153)eV$$

The value of τ_t is similar to the previously obtained values but when compared with the literature value[11] of 0.264ns , there seems to be room for lot of error. The three lifetimes τ_0, τ_t and $\bar{\tau}$ mean are all co-related, so significant errors in any of these might be magnified in the self consistency check.

B. Enthalpy of the vacancy formation

From the sigmoidal fit the Enthalpy of formation was found to be (0.5826 ± 0.0153) eV but from equation (12), the enthalpy can be found from the linear fit which always gives higher confidence levels.

On taking the logarithm of equation (12) and plotting the Arrhenius diagram with linear fit the plot shown in Figure 15 is obtained. From the slop of the fit the Enthalpy of formation is calculated as:

$$H_t = (0.525 \pm 0.044)eV$$

The literature value[11] is found to be $H_t = (0.54 \pm 0.03)eV$ which is close to the calculated values we obtained. The error for 1/T is computed as

$$\Delta\left(\frac{1}{T}\right) = \frac{\Delta T}{T^2} \qquad (15)$$

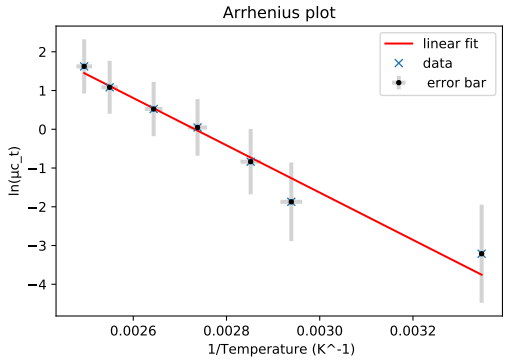

FIG. 16. Arrhenius diagram for the derivation of the enthalpy of the vacancy formation

and the errors for $ln\mu c_t$ is compared according to: $\Delta ln\mu c_t$

$$= \sqrt{\left(\frac{(\tau_t - \tau_f)\Delta\bar{t}}{(\tau_f - \bar{\tau})(\bar{\tau} - \tau_t)}\right)^2 + \left(\frac{\tau\bar{\Delta}\tau_f}{\tau_f^2 - \tau_f\bar{\tau}}\right)^2 + \left(\frac{\Delta\tau_t}{\bar{\tau} - \tau_t}\right)^2} \quad (16)$$

V. RESULTS CONCLUSIONS

In this experiment the life time spectra of positron at different temperatures in an Indium sample were taken using fast-slow coincidence circuit and analyzed with python programming langauge.The reduced χ^2 of the fitting were quite good (≈ 1) as shown in Table 3. The positrons could be trapped in the metal defects and the enthalpy of vacation formation were measured using two methods. The enthalpy of vacancy formation H_t was found as:

- $H_t = (0.5826 \pm 0.0153)eV$ using sigmoidal fit
- $H_t = (0.525 \pm 0.044)eV$ using slope of the Arrhenius diagram

The two values are fairly close and are in the same order of literature values[11]. Thus we conclude that the metals consists of defects such as vacancies, interstitials etc. The positron may annhilate promptly with the free electron giving two γ-ray each of energies of 511 keV in opposite direction or it may be trapped in the defects leading to the increased lifetime of the positrons.

VI. ACKNOWLEDGMENTS

We wish to acknowlede Yannick Wunderlich for his helpful guidelines during the experiment.

[1] Advaned Lab Course, Instruction manual for K225 experiment/
[2] https://www.sciencegateway.org/isotope/sodium.html
[3] McKee, B. T. A., W. Triftshäuser, and A. T. Stewart. "Vacancy-formation energies in metals from positron annihilation." Physical Review Letters 28.6 (1972): 358
[4] Wikipedia, Johnson Filter system https://en.wikipedia.org/wiki/UBVphotometricsystem
[5] F Tuomisto Experiment and theory of positron annihilation
[6] Positron Annihilation Spectroscopy at the HZDR https://www.hzdr.de/db/Cms
[7] A.Belaidi, Positron trapping in some metals, Volume 27, Issue 1, Pages 55-60, January 1991
[8] LYSO Scintillation Material https://www.crystals.saint-gobain.com/products/
[9] https://en.wikipedia.org/wiki/Photomultiplier/tube
[10] Marwan Al-Haik, Effect of Microstructural Variation on the Photo and Radioluminescence of YO:Eu Complexes, January 2011
[11] Weiler, W., and H. E. Schaefer. "Vacancy formation in indium investigated by positron lifetime spectroscopy." Journal of Physics F: Metal Physics 15.8 (1985): 1651.